Supplementary Information (SI) for Journal of Materials Chemistry A.

Supplementary material

Bifunctional NiS_2@MXene Composite Separator for High-Performance Lithium-Sulfur Batteries with Enhanced Polysulfide Inhibition and Uniform Lithium Ion Transport

Bo Zhang, Jiyuan You, Peng Liu, Yuqian Li*, Wenju Wang*
1 School of Energy and Power Engineering, Nanjing University of Science and Technology,
Nanjing 210094, China

4.Experimental

4.1. Synthesis of MXene

To prepare $Ti_3C_2T_x$ (MXene)powder, 1 g of Ti_3AlC_2 MAX powder was gradually introduced into a 30 wt % HF solution and stirred at room temperature for 8 hours under an argon protective atmosphere. The obtained $Ti_3C_2T_x$ powder underwent multiple rinses with deionized water followed by centrifugation at 10,000 rpm for 10 minutes until reaching a neutral pH. Subsequently, the powder was gathered, dried in a vacuum oven at 60 °C to remove any residual moisture.

4.2. Synthesis of Ni@MXene

Initially, 0.1 g of Mxene was dispersed in 60 ml of ethylene glycol, followed by the addition of 0.12 g of $NiCl_2 \cdot 6H2O$ and 0.39 g of $CH_3COOHNH_4$. After stirring for 30 minutes, the mixed solution was transferred to a hydrothermal kettle with a Teflon liner and allowed to react at 180°C for 10 hours. The resulting product was then washed multiple times before being placed in a vacuum drying oven overnight to yield Ni@MXene.

4.3. Synthesis of NiS_2@MXene

Ni@MXene and sulfur powder were mixed in a 1:2 atomic ratio. The mixture was thoroughly ground for 30 minutes before being transferred to a sealed hydrothermal

---

* Corresponding author. E-mail address: wangwenju@njust.edu.cn; wangwenju1982@163.com;

* Corresponding author. E-mail address: liyuqian@njust.edu.cn;

kettle and maintained at 170°C for 10 hours, followed by natural cooling to room temperature. The resulting product was collected, washed with carbon disulfide and anhydrous ethanol to eliminate sulfur powder and any residues, then dried under vacuum at 60°C for 6 hours to yield NiS_2@MXene powder.

4.4. Preparation of NiS_2@MXene coated separator

To prepare the NiS_2@MXene hybrid coating via vacuum-filtration, NiS_2@MXene, carbon black, and binder were dispersed in ethanol (50 mL) solution at a mass ratio of 7:2:1, sonicated for 30 minutes, and then filtered through a commercial separator (porous polypropylene (PP) membrane, Celgard 2400). The entire experiment was carried out under an Ar atmosphere for protection. After placed 12 hours in a vacuum oven set to 60 °C, the coated separator was removed and cut into round disks with a diameter of 1.9 cm. Celgard 2400 separator was utilized as a reference sample for comparison. MXene separator was synthesized according to the similar process to NiS_2@MXene.

4.5. Preparation of sulfur cathode

The sulfur cathode was made using a melt diffusion method. The mass ratio of carbon nanotubes to sulfur was determined to be 1:3. The homogeneous mixture was placed in the ampoule container, sealed, and transferred to the tube furnace. The mixture was then heated to 155 °C at a rate of 1 °C/min in a nitrogen environment and maintained at that temperature for 12 hours. CNT/S was tested with TGA, and the sulfur content was 75.7 %, as shown in **Figure S20**. The CNT/S compound, carbon black, and binder were combined in an 8:1:1 mass ratio. The combination was completely grounded in deionized water and then coated with a two-sided carbon layer on aluminum foil. Finally, the aluminum foil was dried for 12 hours at 50 °C in a vacuum drying oven. Following that, the dry foil sheet was cut into 12 mm disks to use as a backup.

4.6. Assembly of Li-S batteries

CR2032 cells were assembled in a high-purity argon glove box which H_2O and O_2 contents were less than 0.01 ppm. The pole pieces prepared in 2.3 were used as the cathode and the lithium metal pieces were used as the anode. The electrolyte was made up of 1.0 M lithium bis (tri-fluoromethanesulfone) imide (LiTFSI) and 1.0 wt% LiNO3 dissolved in 1, 3-dioxolane (DOL) and dimethoxymethane (DME).

4.7. Characterizations

In an argon environment, the CNT/S compound was heated from 25 °C to 600 °C at a rate of 5 °C/min to determine the sulfur mass content. Powder X-ray diffraction (XRD) patterns were acquired using a Rigaku D/max-2500 apparatus (40 kV, 100 mA) with a Cu/Ka X-ray source at a scanning rate of 3.0°/min spanning the 10°-80° range. The microstructure of samples was investigated using a scanning electron microscope (SEM). The valence states and electronic orbitals of elements in materials are determined using X-ray photoelectron spectroscopy (XPS). Transmission electron microscopy (TEM) and high-angle annular darkfield scanning transmission electron microscopy (HAADF-STEM) were used to investigate the internal morphology of materials. Simultaneously, the elemental composition of the sample material was measured using energy dispersive X-ray spectroscopy (EDS). For the specific surface area and porosity distribution measurement, the N_2 adsorption/desorption isotherm was carried out at 77 K. The LAND CT2001A battery test apparatus (LANHE, China) was used to evaluate cells with a variety of separators. The cutoff voltage was set at 1.7-2.8 during the test. Additionally, cyclic voltammetry (CV) and electrochemical impedance spectroscopy (EIS) were used to evaluate the electrochemical performance of the cell. Finally, the pouch cell was constructed to demonstrate the utility of the material. Li_2S deposition experiments were conducted to investigate the transformation of polysulfides on different material surfaces. The cell was firstly discharged at a constant current of 0.112 mA to 2.06 V and subsequently discharged at a constant voltage of 2.05 V until the current decreased below 0.001 mA.

4.8. Preparation of polysulfide solution

To avoid the concentration changing of Li_2S_6 solution during long-term storage, we prepared a fresh Li_2S_6 solution. The preparation method is as follows: The preparation of Li_2S_6 solution is all operated in an inert atmosphere. First, S_8 and Li_2S were added to a mixed solution of DOL/DME (v/v = 1:1) at a molar ratio of 5:1, followed by magnetic stirring at 50°C for 24 hours to obtain the 0.5 M, 5×10^{-2} M and 5×10^{-4} M Li_2S_6 solutions. In addition, we also configured Li_2S_8/Tetraglyme solution. S_8 and Li_2S were added to the solution of Tetraglyme with 1 M LiTFSI at a molar ratio of 5:1, followed by magnetic stirring at 60 °C for 24 hours to obtain the 0.5 M Li_2S_8 solution.

4.9. The coefficient calculation of Li-ion diffusion

According to the Randles-Sevick equation:

$$i_p = (2.69 \times 10^5)\, n^{3/2}\, A\, D_{Li^+}^{eff\,1/2}\, v^{1/2}\, C_{Li^+} \qquad \text{(S1)}$$

(1) Measure the cyclic voltammogram of the material at different scan rates, then graph the peak current as the Y-axis and the square root of the scan rate as the X-axis, fit the curve and find out the slope to obtain

$$K = i_p / v^{1/2} \qquad \text{(S2)}$$

(2) Bringing each data into the calculation, you may wish to set

$$L = (2.69 \times 10^5)\, n^{3/2}\, A\, C_{Li^+} \qquad \text{(S3)}$$

where i_p is the peak current (A); n is the number of electron transfers involved in the electrochemical reaction process, here taken as 2; A is the anode area (cm^2), here taken as 1.13; $D_{Li^+}^{eff}$ is the Li-ion diffusion coefficient, $cm^2\, s^{-1}$; C_{Li^+} is the Li-ion concentration in the cell ($mol\, L^{-1}$); v is the scan rate ($V\, s^{-1}$).

Therefore:

$$D_{Li^+}^{eff} = (K/L)^2 \qquad \text{(S4)}$$

Table S1 D_{Li+} of NiS_2@MXene, MXene, and pristine separator cells

Parameters	Peak A	Peak B	Peak C
NiS_2@MXene	1.2774×10^{-7}	2.0635×10^{-8}	2.1101×10^{-8}
MXene	1.1798×10^{-7}	1.3599×10^{-8}	1.9774×10^{-8}
Pristine	7.2274×10^{-8}	5.6632×10^{-9}	1.4169×10^{-8}

4.10. Simulation of ion transport and deposition processes

The lithium deposition transient model constructed in this study is based on a neutral electrolyte environment, in which the electrolyte primarily contains Li^+ and the anion A$^-$. The model assumes that the electrolyte is completely dissociated and that the proton concentration is negligible, thereby excluding any proton material balance. Furthermore, both the anode and cathode current efficiencies are set to 100% to eliminate the effects of side reactions. Although the deposition process may induce an electrolyte density gradient, the natural convection effect caused by the concentration gradient can be neglected within the simulation parameters. During the simulation, the controlling equations for ion fluxes are described by the Nernst-Planck equation (S5):

$$\boldsymbol{N}_i = - D_i \nabla c_i + z_i u_i F c_i \nabla \phi_l$$

(S5)

Here, the fluxes for Li$^+$ and A$^-$are calculated separately, where z_i denotes the ion charge (Li$^+$: +1, A$^-$: –1), N$_\mathrm{i}$ is the transfer vector (mol (m^2·s)$^{-1}$), c_i is the electrolyte concentration (mol·m^{-3}), u_i represents the mobility of the charged species (m^2 (s·J·mole)$^{-1}$), F is the Faraday constant (As mole^{-1}), and ϕ_l is the electrolyte potential (V). The material conservation equation is expressed as:

$$\frac{\partial c_i}{\partial t} + \nabla \cdot \boldsymbol{N}_i = 0$$

(S6)

The electroneutrality condition is enforced by:

$$\sum z_i c_i = 0$$

(S7)

The anodic boundary, which governs the lithium deposition kinetics, is described by the modified Butler-Volmer equation:

$$\boldsymbol{N}_{Li^+} \cdot \boldsymbol{n} = - \frac{i_0}{F}\left[exp\left(\frac{\alpha_a F \eta}{RT}\right) - \frac{c_{Li^+}}{c_{ref}} exp\left(- exp\left(\frac{\alpha_c F \eta}{RT}\right)\right]$$

(S8)

where the overpotential is defined as:

$$\eta = \phi_s - \phi_l - \Delta\phi_{eq}$$

(S9)

The negative electrode boundary is treated analogously to the lithium dissolution process, while the insulating boundary condition satisfies:

$$\boldsymbol{N}_{Li^+} \cdot \boldsymbol{n} = \boldsymbol{N}_{A^-} \cdot \boldsymbol{n} = 0$$

(S10)

The initial electrolyte concentration is uniformly distributed as follows:

$$c_{Li^+} = c_{A^-} = c_0 \tag{S11}$$

The model employs the “Cubic Current Distribution, Nernst-Planck Equation” interface, and the “Deformation Geometry” node is used to track mesh deformation. By using the “Electrode Surface” boundary node and incorporating dissolved-deposited material, the ionic fluxes and boundary mesh velocities depend on the reaction current, the number of electrons, and the specified stoichiometric coefficients of the electrode reactions. The overall reaction is simplified as:

$$Li^+ + e^- \rightarrow Li \tag{S12}$$

which corresponds to stoichiometric coefficients of v_{Li+}=-1 and v_{Li}=1.

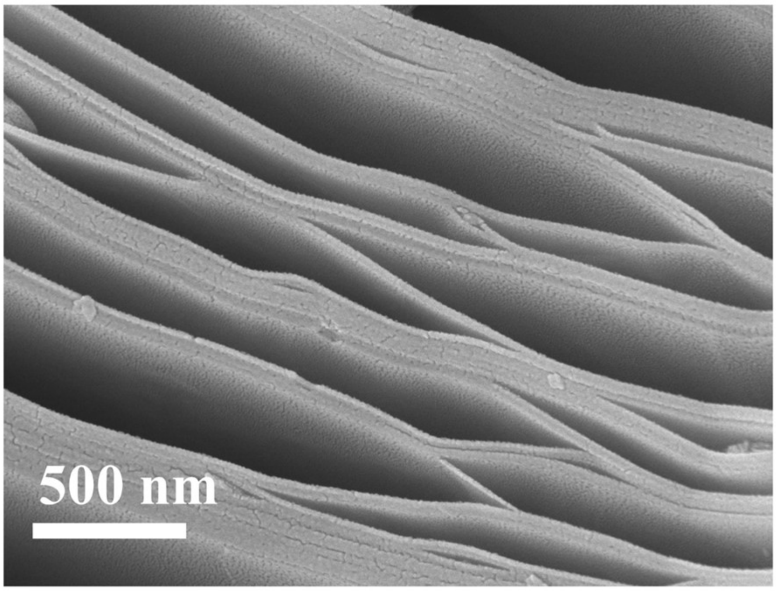

Figure S1. SEM image of the MXene

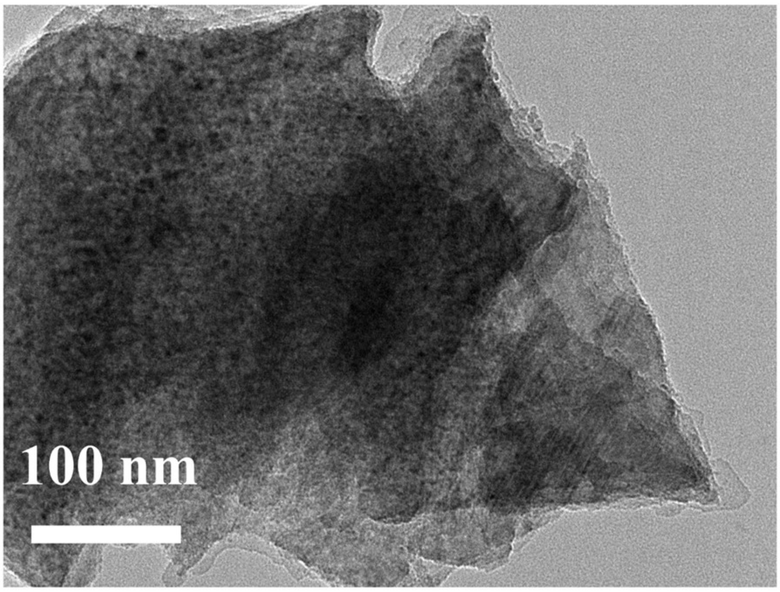

Figure S2. TEM image of the Mxene

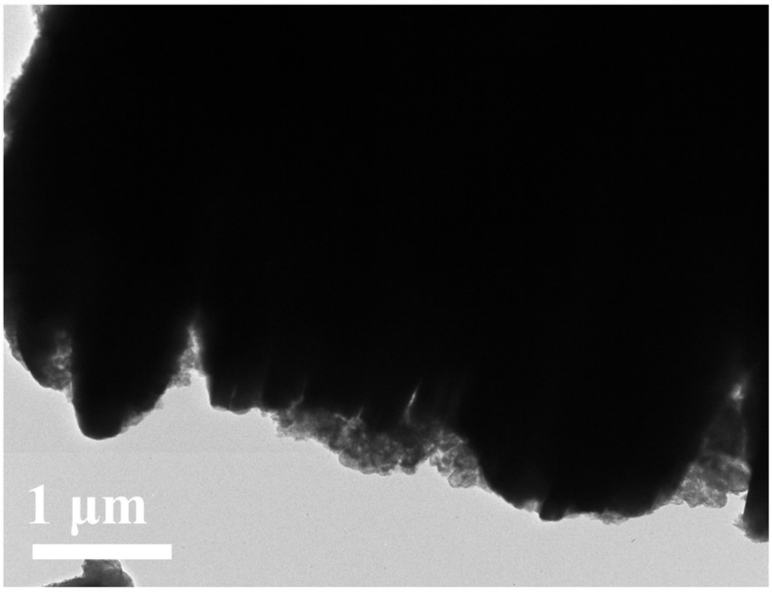

Figure S3. TEM image of the NiS_2@Mxene

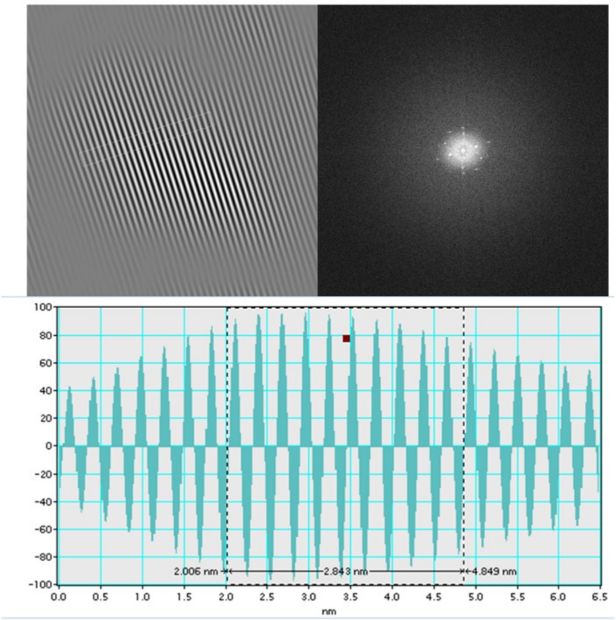

Figure S4. The procedure for calculating the lattice spacing

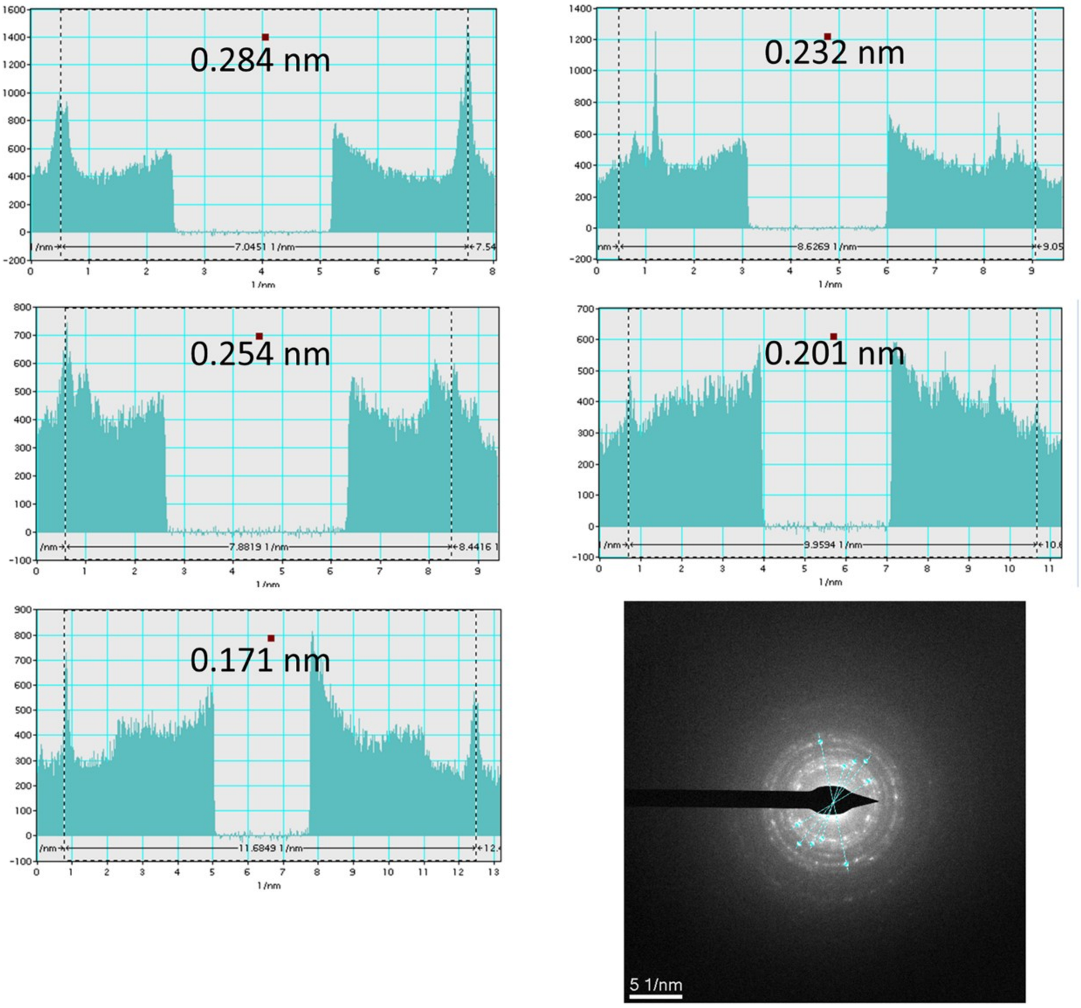

Figure S5. The procedure for calculating the lattice spacing

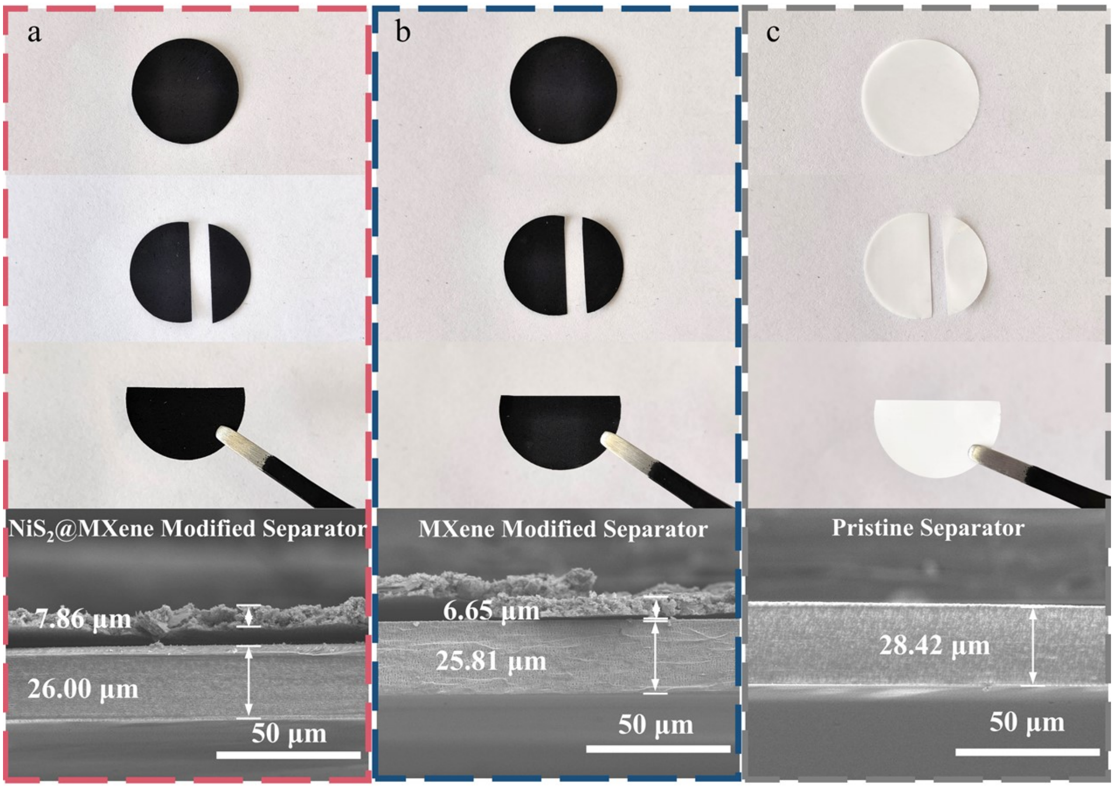

Figure S6. EM images of (a) NiS_2@MXene modified separator, (b) MXene modified separator and (c) pristine separator, along with their corresponding cross-sectional SEM images.

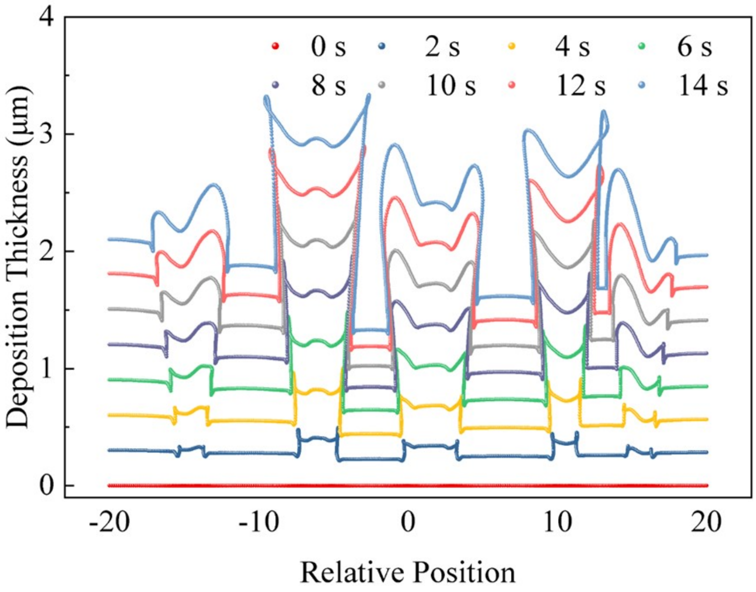

Figure S7. Lithium deposition growth curves under the influence of the pristine separator.

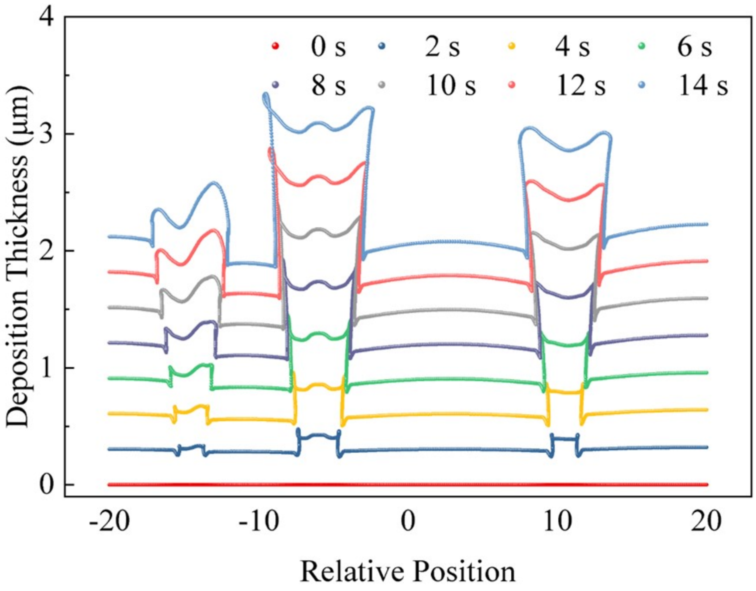

Figure S8. Lithium deposition growth curves under the influence of the MXene separator.

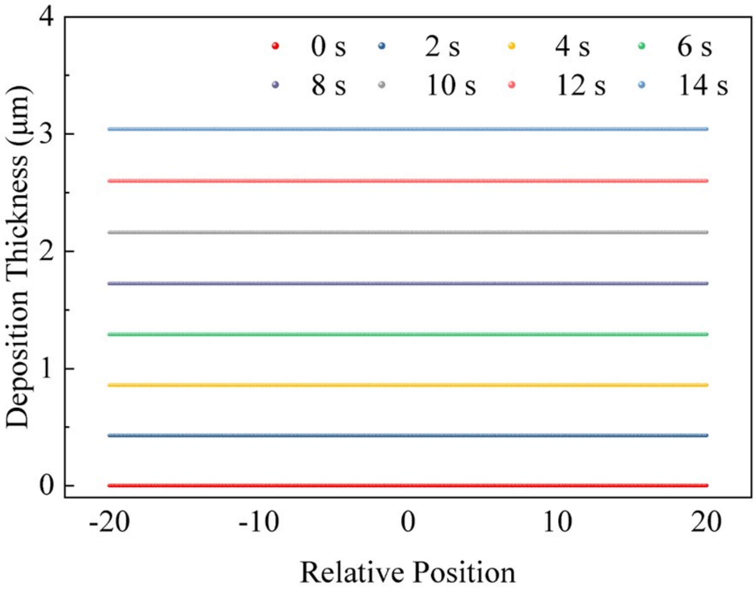

Figure S9. Lithium deposition growth curves under the influence of the NiS_2@MXene separator.

Figure S10. Contact angle test results of the NiS$_2$@MXene separator.

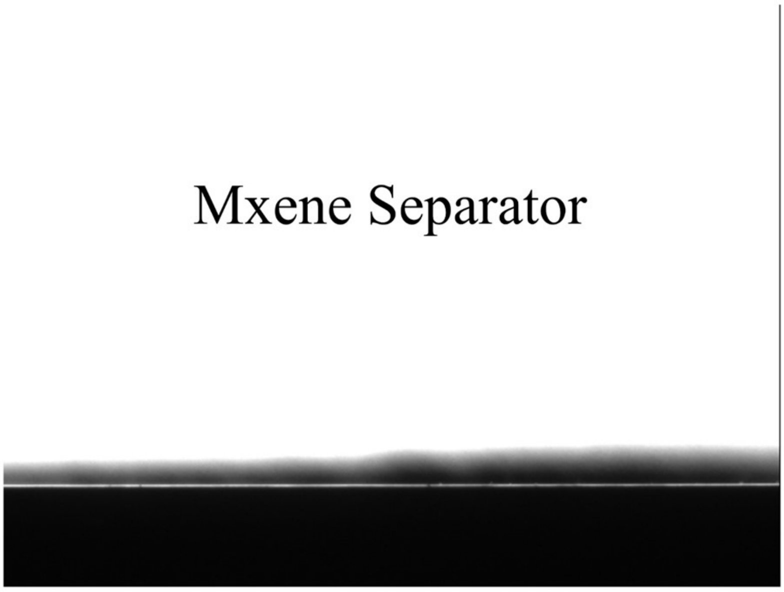

Figure S11. Contact angle test results of the MXene separator.

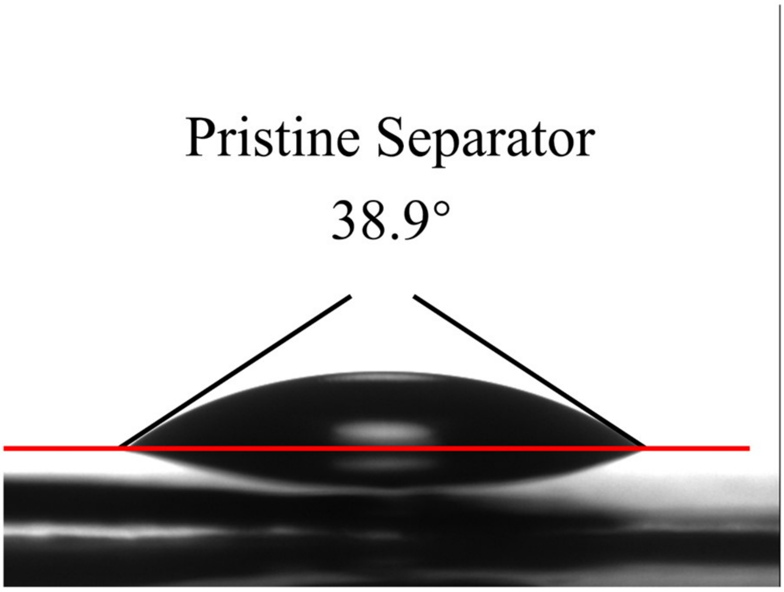

Figure S12. Contact angle test results of the Pristine separator

Table S2. The fitting data of EIS curves.

Separator	**R_s(Ω)**	**R_{ct}(Ω)**
NiS_2@MXene separator.	2.557	43.99
MXene separator.	2.875	44.54
Pristine separator	2.947	56.4

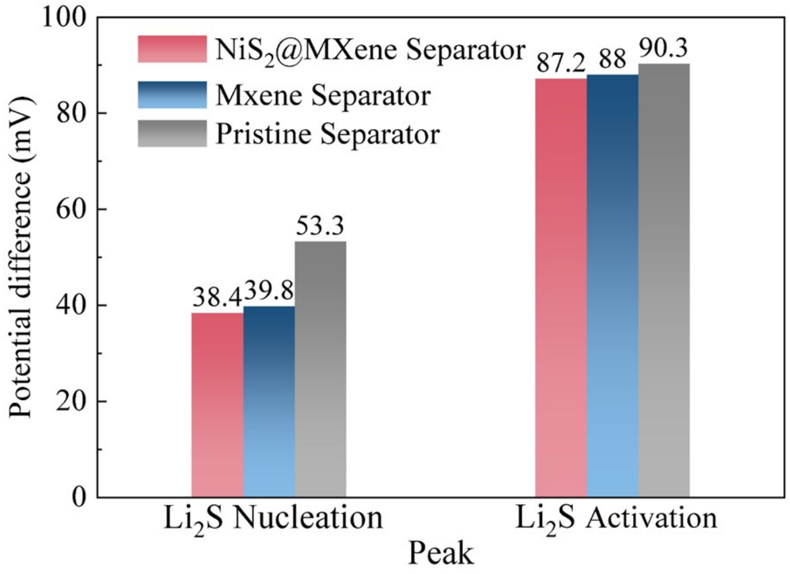

Figure S13. ΔIR of three cells.

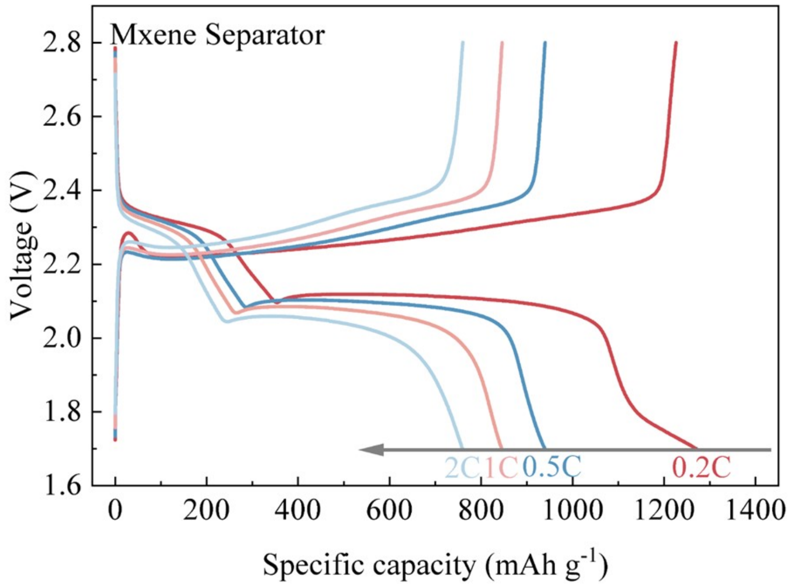

Figure S14. Charge-discharge profiles of rate of the cell with MXene separator.

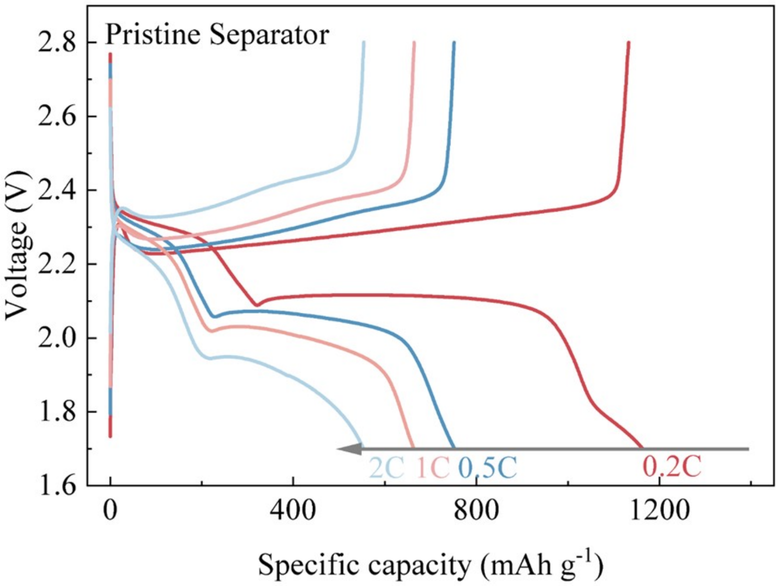

Figure S15. Charge-discharge profiles of rate of the cell with Pristine separator.

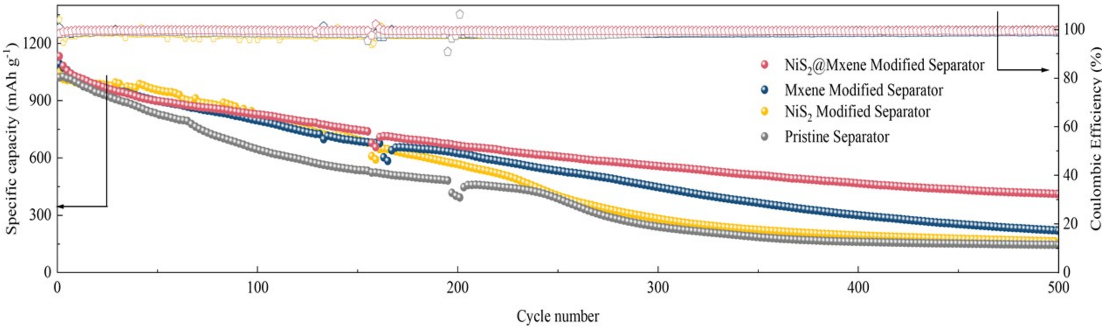

Figure S16. Long-term test results of NiS$_2$@MXene modified separator cell, NiS$_2$ modified separator cell, MXene modified separator cell and pristine separator cell.

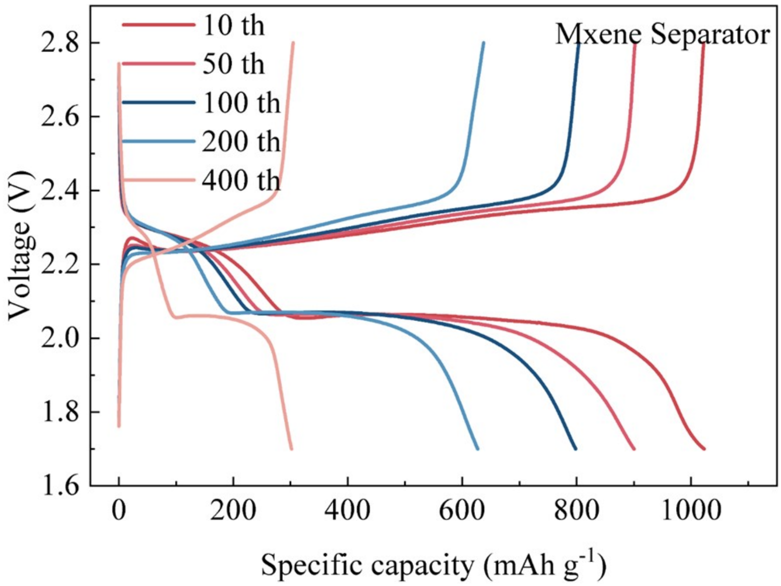

Figure S17. Charge-discharge profiles of different cycle of the cell with Mxene separator.

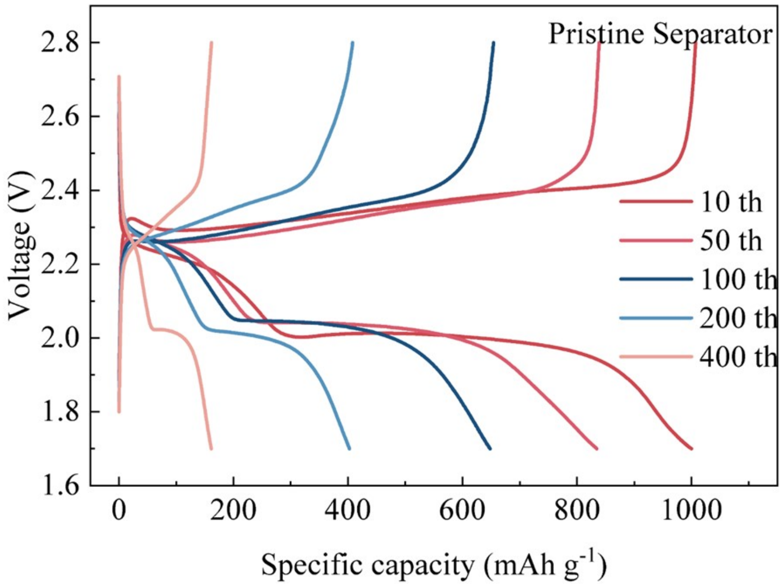

Figure S18. Charge-discharge profiles of different cycle of the cell with Pristine separator.

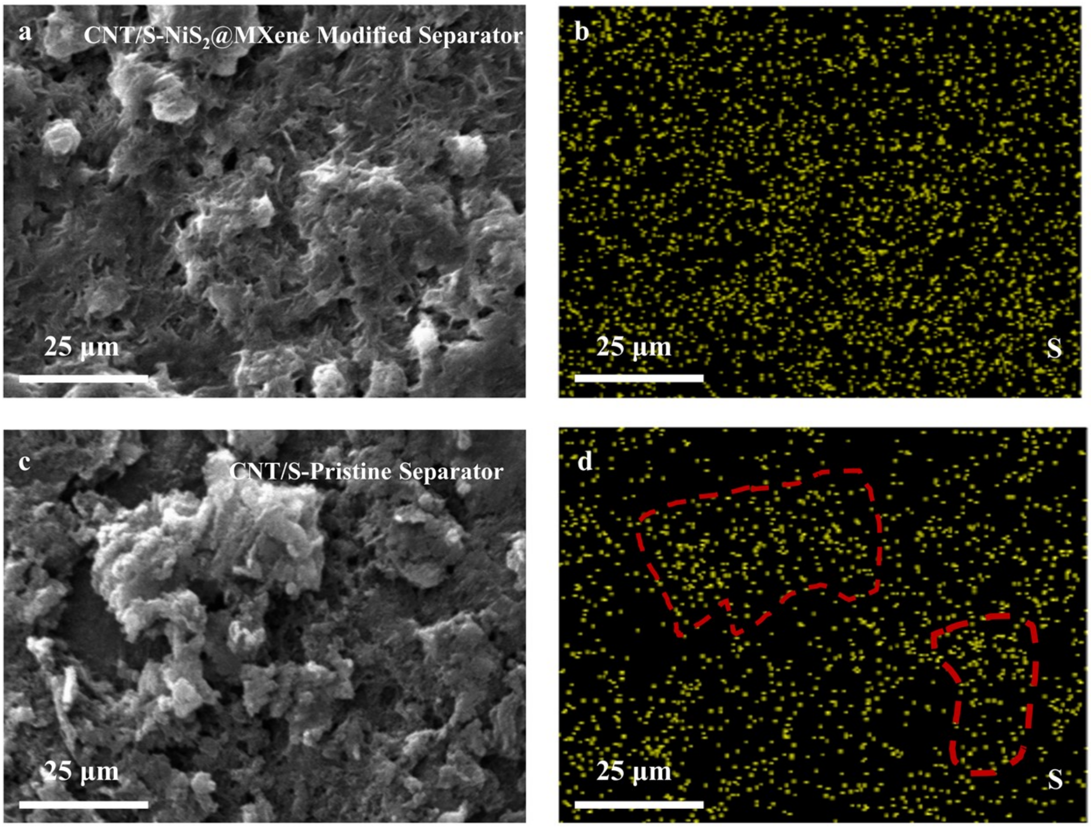

Figure S19. SEM and EDS images of cathodes from cells with (a-b) NiS$_2$@MXene modified and (c-d) pristine separators after long-term testing.

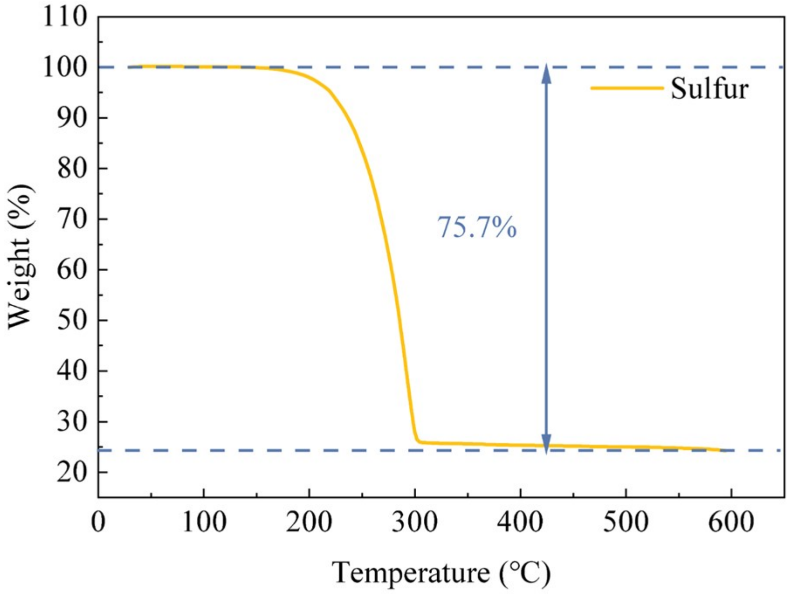

Figure S20. The TG curve of CNT/S composite cathode.